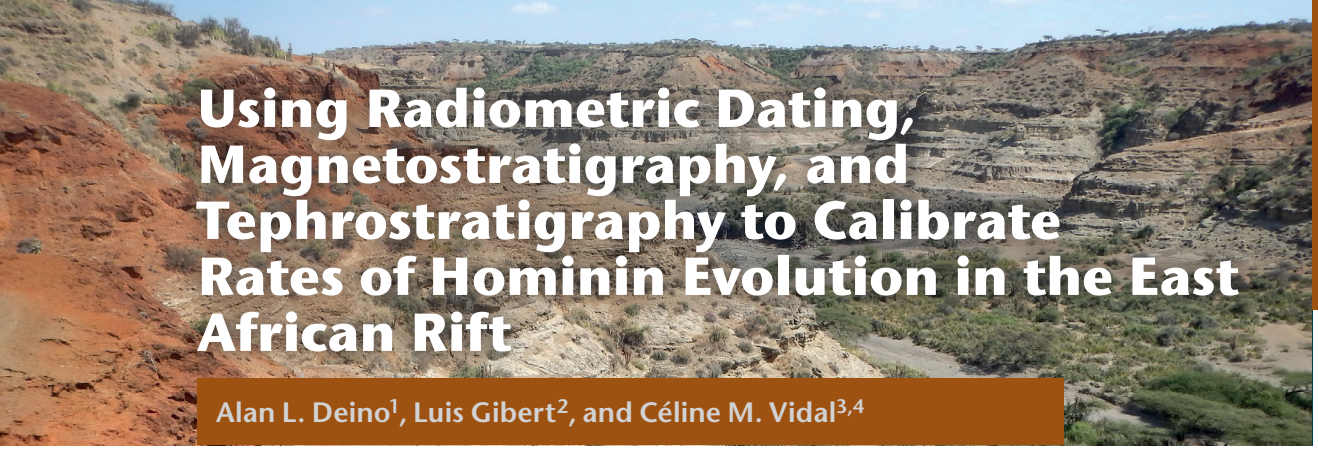

Using Radiometric Dating, Magnetostratigraphy, and Tephrostratigraphy to Calibrate Rates of Hominin Evolution in the East African Rift

Alan L. Deino[1], Luis Gibert[2], and Céline M. Vidal[3,4]

Olduvai Gorge, Tanzania. Looking west from Locality 27, near the eastern limit of the gorge. The reddish to brownish strata are Beds II (~1.8–1.1 Ma) and III (~1.1–0.9 Ma), overlying the white to grey Bed I (~2.0–1.8 Ma).

1811-5209/23/0019-0088$2.50 DOI: 10.2138/gselements.19.2.88

Age-calibration of hominin fossils and artifacts in the East African Rift is principally achieved through dating of associated volcanic-sedimentary strata. The dominant dating techniques for sites ≥100 ka are the $^{40}Ar/^{39}Ar$ radiometric dating method, magnetostratigraphy, and tephrostratigraphy. The $^{40}Ar/^{39}Ar$ technique relies on the occurrence of volcanic deposits in the target strata, which are often present as a consequence of the interplay of rift formation and volcanic activity. The frequency of datable material may be limited; however, by also applying the relative dating methods of magnetostratigraphy and tephrostratigraphy to these same strata, a chronostratigraphic framework can be built and applied to fossiliferous strata. This chapter provides examples of the application of these techniques at Olduvai Gorge, Tanzania, and two areas of the East African Rift in Ethiopia.

KEYWORDS: East Africa Rift; tephrostratigraphy; magnetostratigraphy; $^{40}Ar/^{39}Ar$ dating; paleoanthropology; archeology; tephrochronology

INTRODUCTION

The geological investigation of hominid fossil finds in eastern Africa has a long history, beginning with Hans Reck at Olduvai Gorge, Tanzania, in 1913, and the renewed geological, paleoanthropological, and archeological investigations at Olduvai by Richard and Mary Leakey, Richard Hay, and others beginning in the 1930s. The first absolute age calibration of hominid fossils in the rift was undertaken on the Olduvai stratigraphic sequence. Using the K–Ar method, Jack Evernden and Garniss Curtis (Leakey et al. 1961; Evernden et al. 1965) produced age measurements for "*Zinjanthropus*" (now *Paranthropus boiseii*) of ~1.75 Ma that proved quite controversial (potentially doubling or tripling the duration of the Pleistocene and placing the strata in a much older context than anticipated), yet these ages have withstood the test of time and are quite close to modern $^{40}Ar/^{39}Ar$ ages for Olduvai Bed I.

Since these early beginnings, geological investigations of hominid fossils in the East African Rift have expanded to many sites in Tanzania, Kenya, and Ethiopia. In light of the significance of such finds to human origins, intensive geological investigations have been conducted at these sites, seeking to thoroughly define the stratigraphic and structural setting. This work has been complemented by efforts to precisely determine the ages of finds and their associated stratigraphy, often with the goal in mind of providing a paleoenvironmental context to the progress of human evolution.

Comprehensive age calibration of sedimentary strata in the rift can be viewed as three legs of a tripod—radiometric dating, magnetostratigraphy, and tephrostratigraphy. Radiometric dating in practice, in the rocks of interest of the Middle–Late Cenozoic, is reliant on the $^{40}Ar/^{39}Ar$ dating technique in the East African Rift setting. Volcanic rocks are fairly ubiquitous in the rift, though occasionally sparse. The pyroclastic component of this volcanism forms the basis of the tephrostratigraphic relative-dating approach. Paleomagnetism can of course be applied to sedimentary strata within or outside of a rift setting, but the availability of one or more volcanic horizons that are radiometrically or tephrostratigraphically datable provides a necessary basis to anchor the magnetostratigraphy to the global paleomagnetic timescale.

$^{40}AR/^{39}AR$ DATING

The $^{40}Ar/^{39}Ar$ radiometric dating method provides a widely applicable, accurate means for the age calibration of hominid evolution in the context of the East African Rift. This method is a variant of the K–Ar technique, which utilizes the spontaneous decay of radioactive ^{40}K (about 0.012% of all K in nature) in rocks and minerals to daughter products, mostly ^{40}Ca, but ~10% of the time to the product of interest, ^{40}Ar. The half-life of ^{40}K decay is 1.25 billion years. While this rate may appear low in relation to events on the human evolution timescale, because of the high abundance of potassium in crustal materials with suitable mineral and rock phases, events as young as a few thousand years can be accurately dated with modern mass spectrometers and procedures. The assumptions behind the use of this decay scheme to date rocks are (1) that the material to be dated has an identifiable starting point with virtually zero trapped ^{40}Ar and (2) that the ^{40}Ar generated by

1 Berkeley Geochronology Center
Berkeley, CA, USA
E-mail: alan.deino@gmail.com

2 Dept. of Mineralogy, Petrology and Applied Geology
Faculty of Earth Sciences
University of Barcelona
Martí Franquès s/n
08028 Barcelona, Spain
E-mail: lgibert@ub.edu

3 Fitzwilliam College
Storey's Way
CB3 0DG Cambridge, United Kingdom
E-mail: cv325@cam.ac.uk

4 University of Cambridge
Department of Geography
Downing Place
CB2 3EN Cambridge, United Kingdom

^{40}K decay events remains quantitatively trapped within the host material over geological time. In practice, these assumptions are best met in volcanic materials; upon eruption and initial cooling, vanishingly small quantities of ^{40}Ar are trapped, whereas over geologic time, ^{40}Ar remains a closed system in unaltered crystalline materials such as feldspar and biotite.

In the ^{40}Ar/^{39}Ar variant of the K–Ar technique, purified samples are first irradiated in the core of a nuclear reactor to convert some of the naturally occurring ^{39}K to ^{39}Ar by bombardment with fast neutrons. Irradiation is typically performed in one of several available research reactors for anywhere from a few minutes to tens of hours for samples of Cenozoic age. The ^{40}Ar/^{39}Ar dating method requires calibration of the neutron flux of the irradiation to calculate an age, which is achieved by the co-irradiation of geological materials of known age in close physical proximity to the unknowns (the reader is referred to an excellent reference by McDougall and Harrison (1999) for a detailed exposition on the theory and calculations underlying the ^{40}Ar/^{39}Ar dating method). Two commonly used reference materials (age standards) for Cenozoic work are phenocrystic sanidine from the Fish Canyon Tuff of Colorado, USA (orbitally referenced age of 28.201 ± 0.046 Ma; Kuiper et al. 2008) and sanidine from the Alder Creek Rhyolite of California, USA (1.1848 ± 0.0006 Ma; Niespolo et al. 2017). These standard ages are known precisely enough that they rarely play a significant part in the uncertainty of the overall geological interpretation in hominid dating circumstances.

Following a "cooling" period of several weeks to months (depending on the length of the irradiation and the material irradiated), the irradiated material is analyzed under ultra-high vacuum conditions. Lasers are typically used to outgas the material to release trapped argon, although an electrical resistance furnace can be used for larger samples (e.g., >100 mg). Samples can be quickly heated to fusion to release all of the trapped argon in one experiment, i.e., the "total-fusion" approach, or can be incrementally heated using lasers that have rampable power control. After the release of the gas from the sample, extraneous reactive species (e.g., H_2O, CO_2, CO, NO, H) are removed via getters and cold traps within a period of several minutes. After cleanup, the gas is admitted to a noble-gas mass spectrometer for measurement of five argon isotopes (^{40}Ar through ^{36}Ar), after which the age can be calculated.

Most high-K phases such as sanidine, anorthoclase, and biotite are preferably dated by experiments involving a single grain, but small grain populations are sometimes utilized for lower-K materials (<2% K), fine grain sizes (i.e., <300 µm), or young materials (<0.001–1 Ma). Mafic lavas can be dated using small aliquots of groundmass or whole-rock material, although these may be subject to complications arising from very fine internal grain sizes (recoil loss and Ar diffusion) or multi-component complexities to interpreting Ar release spectra.

One of the greatest advantages of the ^{40}Ar/^{39}Ar technique is that the K and Ar abundances are determined for the same material at the same time. Thus, with sensitive mass spectrometers and precise heating devices (i.e., ramping of power output of CO_2 lasers), the technique can resolve precise ages down to the individual grain level, and with incremental heating, even sub-grain-level age information can be inferred.

Calibrating human evolution in the East African Rift usually involves dating volcanic rocks interbedded with fossiliferous or archaeological depositional sites. Relatively high precision can be attained by dating unaltered K-feldspar phenocrysts extracted from pumice in primary tuffs; in the late Cenozoic, dating of such materials can yield ±0.1% precision. Many circumstances are less opportune, however, involving reworked tephra or lower-K materials (e.g., plagioclase, basalts). Biotite may be the sole potassic mineral in carbonatitic or undersaturated volcanic rocks in parts of the rift, and while K is abundant, these minerals are phyllosilicates and their sheet-like structures are susceptible to alteration along interlayer bonds, resulting in post-depositional K and potentially Ar exchange with the environment. Minerals with lower K, such as plagioclase and hornblende, can be dated depending on their age, grain size, and K content.

The most optimal conditions for accurate dating in a paleoanthropological setting in the rift involves pyroclastic deposits (e.g., fallout, primary ignimbrites, or rapidly reworked but largely uncontaminated tuffs) that tightly bracket the target horizon in an unweathered, continuous stratigraphic sequence. For the best results, these pyroclastics should contain K-feldspar phenocrysts (sanidine or anorthoclase), dated using the single-grain approach, either through total-fusion or incremental heating. Given these constraints, late Cenozoic ages with precision less than ±1% are fairly routine and extend down to as low as 0.1%. Complications arise from contamination with older material (either incorporated during eruption, or from fluvial processes in the case of reworked tuffs), or because of the presence of "initial" Ar present within the crystals upon eruption and incompletely outgassed prior to emplacement.

While our discussion has focused on ^{40}Ar/^{39}Ar dating, it is important to keep in mind that other absolute dating techniques are frequently utilized for rocks of Late Pleistocene (<129 ka) or Holocene age. These include the rapidly evolving variants of the luminescence technique, and ^{14}C dating.

^{40}Ar/^{39}Ar Example—Chronostratigraphy of Drill Cores from Olduvai Basin, Tanzania

An example of application of the ^{40}Ar/^{39}Ar dating technique in the East African Rift is provided by a recent study of a set of drill cores recovered from mostly fluviolacustrine and fan-delta volcaniclastic Pleistocene strata at three sites in the Olduvai Basin, Tanzania (e.g., McHenry et al. 2020; Stanistreet et al. 2020; Deino et al. 2021). These cores (a total core length of 611.72 m, with 575.48 m recovered) were drilled in 2014 as part of the Olduvai Gorge Coring Project for the purposes of refining the stratigraphy and paleoclimate of the basin.

The Olduvai Gorge is a fluvial incision into Plio–Pleistocene strata composed of fluviolacustrine deposits and intercalated lavas, ignimbrites, fallout tuffs, and volcaniclastic strata, deposited within and adjacent to a saline–alkaline lake and fan-delta volcaniclastic wedge paleoenvironments. The basin sits westward of major faults of the eastern branch of the East African Rift Valley and the adjacent contemporaneous volcanoes of the Ngorongoro Volcanic Highlands (NVH) (Hay 1976). The oldest Pleistocene exposures in the basin are ~2.0-Ma ignimbrites erupted from Ngorongoro Caldera to the east in the NVH. Crystalline basement beneath the sedimentary infill consists of metamorphic rocks of the Archean Tanzanian Craton and the late Proterozoic Pan-African Mozambique Belt.

A chronostratigraphic framework incorporating these cores and outcrop exposures was developed based on ^{40}Ar/^{39}Ar dating of core and outcrop volcanic and volcaniclastic units, core paleomagnetic stratigraphy, and tephrochemical correlation between cores and from core to outcrop (Deino et al. 2021). The ^{40}Ar/^{39}Ar geochronology component of

this study dated 61 core tuff layers, a mafic lava flow from the core, and seven outcrop exposures of tuffs that tie into the core chronostratigraphy. Select tuff layers were dated using the single-crystal, incremental heating approach, usually on anorthoclase but also on sodic plagioclase. The core magnetostratigraphy was determined by the measurement of 535 samples. The $^{40}Ar/^{39}Ar$ ages, measured core magnetostratigraphy, and tephrochemical analyses were synthesized and tied into previously characterized outcrop tuff units, which enables previously determined outcrop geochronology to be incorporated into the core. The resulting dataset, consisting of a set of core depths with known age, was input into a Bayesian stratigraphic age model with the prior constraint that ages must decrease monotonically upward, yielding posterior estimates of absolute ages and uncertainties for all covered core depths (Fig. 1).

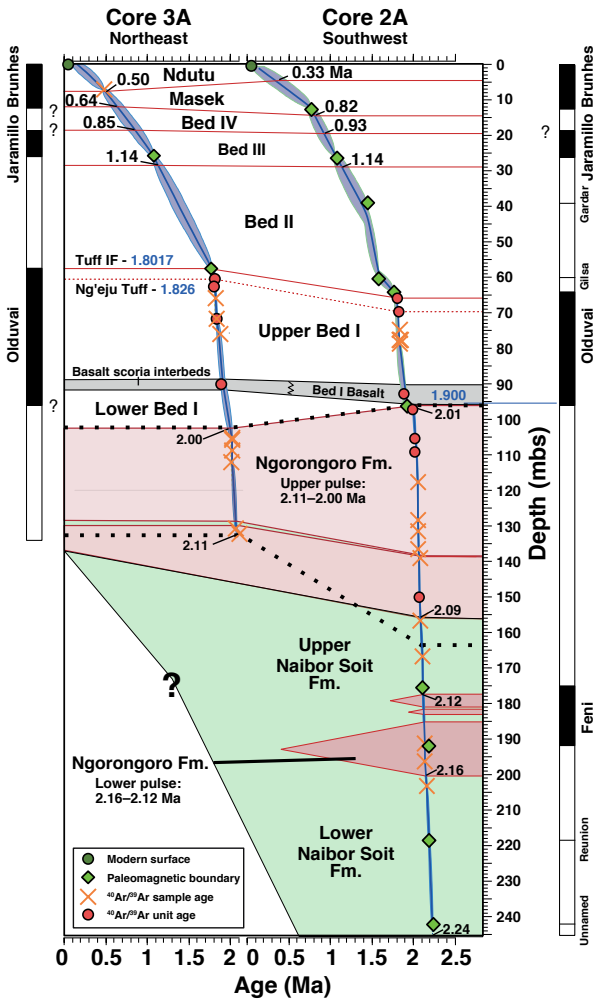

Figure 1 Comparative chronostratigraphy and Bayesian age models of two cores (2A and 3A) from the Olduvai Gorge Coring Project. Lithostratigraphic divisions and nomenclature are shown as most recently revised and expanded by Stanistreet et al. (2020). Core magnetostratigraphies are show to the left and right of the depth profiles. Age models are shown as solid blue lines with 95% confidence intervals. All numbers within the main body of the figure are ages in Ma; those in black are derived from the core Bayesian age models, while those in blue are $^{40}Ar/^{39}Ar$ unit ages. These results illustrate the quality age control provided by combined $^{40}Ar/^{39}Ar$ dating, magnetostratigraphy, and tephra geochemistry, ultimately permitting realistic age estimates for formation boundaries previously difficult to quantify (upper Olduvai units); improved age estimates for zones with sparse age control (i.e., middle to lower Bed I); and age control for strata newly recognized in the core that are below the oldest exposures of Olduvai Gorge.

These models provide age estimates for upper Olduvai Gorge stratigraphic units that have been difficult to date in the past because of the paucity of suitable material for radiometric dating and the absence of detailed magnetostratigraphic investigations. The study also contributes to the overall chronostratigraphic framework of this part of the rift, through correlations between core and outcrop, yielding improved ages for regional tuff units. The study identified possible volcano-tectonic disruptions associated with the buildup and climactic eruption of the nearby Ngorongoro Volcano in the NVH. The coring and dating effort provided a possibly complete history of the buildup of the Ngorongoro Volcano by encountering strata up to ~210 ka older than those exposed in the Gorge. Along with seismic imaging of the basin, extrapolation of Bayesian stratigraphic models suggests that the oldest sedimentary infill on the crystalline basement occurred ~2.5 Ma.

MAGNETOSTRATIGRAPHY

Magnetic polarity stratigraphy (magnetostratigraphy) employs the polarity of the ancient geomagnetic field preserved in sedimentary and volcanic strata to date, correlate, and establish accumulation rates in stratigraphic successions. The geomagnetic polarity timescale (GPTS) is a geo-calendar in which all recognized polarity reversals are dated. Because reversals in the Earth's magnetic field are relatively fast (<5 ky) and synchronous planet-wide, a local magnetostratigraphy can be dated by correlation to the GPTS. The age of geomagnetic reversals is determined by radiometric dating of volcanic rocks close to polarity boundaries, using cyclostratigraphy or calculating ages based on spreading rate models of oceanic crust based on polarity transitions recorded in basalts. Since its initial introduction, the GPTS has undergone extensive refinement, and today, all Cenozoic polarity chrons are calibrated by precise placement within marine cyclostratigraphic sections tied to solar insolation variations (Ogg 2020). Magnetostratigraphy can be especially useful in regions without volcanic deposits, where direct radiometric dating is not possible, though in the East African Rift at least a few datable volcanic horizons are typically present. Magnetostratigraphy also can help produce high-resolution correlations between different sectors of a basin or between marine and terrestrial records. As with all techniques, it has limitations—constructing a reliable magnetostratigraphy requires a succession of rocks with suitable ferromagnetic minerals to record the original magnetic field at the time of deposition. In addition, at least an approximate age for the deposits must be known from radiometric dating, tephrostratigraphy, or biostratigraphy to constrain the possible correlations of the local polarity sequence to the reference GPTS.

The fidelity of the paleomagnetic record in a sedimentary succession is a function of the quality of the magnetic recorders, which improves with high and continuous accumulation rates, relatively fine-grained detrital input, and deposition in a subaerial (oxic) environment. This scenario is found frequently in the East African Rift, hence magnetostratigraphy has been used since the early 1970s for age calibration, including for dating of hominid-bearing strata, to define and calibrate magnetic chrons. As an example, "Olduvai" refers to the early Pleistocene normal polarity chron C2n dated between 1.77 and 1.935 Ma identified at Olduvai Gorge (Grommé and Hay 1971).

Natural remanent magnetization (NRM) refers to the overall magnetization present in a rock. Sedimentary rocks bearing magnetic minerals record the polarity of the Earth's magnetic field during the time of deposition and early diagenesis, while volcanic rocks acquire magne-

tization after ferromagnetic minerals cool below their Curie temperature (specific to each mineral). This initial component of the NRM is called the primary or characteristic remanent magnetization (ChRM). However, rocks may subsequently acquire additional magnetic components during their burial, exhumation, and exposure history. For example, new magnetic minerals can form during diagenesis or weathering processes, and a viscous remanent magnetization can be acquired during extended exposure to the Earth's geomagnetic field. Thus, the NRM is the sum of various magnetic components acquired during and subsequent to the formation of the rock. The only useful magnetization for the purposes of magnetostratigraphy is the ChRM; the other components are secondary and must be subtracted from the NRM. This is achieved via thermal or alternating field stepwise demagnetization (see Langereis et al. 2010 and references therein).

Sampling is a key issue in any magnetostratigraphic study. It is important to select the best available stratigraphic section, which should be as long as possible to record multiple polarity zones, avoid stratigraphic discontinuities, exhibit favorable lithologies, and provide an opportunity to acquire complementary chronological data. The best samples for analysis usually are unweathered fine-grained sediments without late diagenetic effects. Block samples with an oriented face can be collected manually with simple cutting and abrading tools, which may be especially useful with softer rocks. Alternatively, a battery- or gasoline-powered drill can be used to collect oriented cylinders. It is good practice to collect enough material from each sampled strata to perform triplicate measurements, in case some sub-samples prove unsuitable and to demonstrate reproducibility. In the laboratory, samples are cut, surfaces cleaned, and directions measured in a magnetometer at different steps of a demagnetization process. These measurements can be visualized in a Zijderveld diagram showing changes in the intensity and direction of the NRM during the demagnetization process, revealing the different components (Zijderveld 1967) (Fig. 2). The ChRM is usually calculated by means of principal component analysis (Kirschvink 1980). The blocking temperature of a sample and coercivity spectra are used to identify ferromagnetic minerals carrying a ChRM (Lowrie 1990). Field tests of paleomagnetic stability should be carried out to demonstrate that the identified ChRM is the primary component. A fold test is commonly performed, when possible, which determines whether the paleomagnetic directions are grouped as expected after correction for the stratigraphic tilt or have divergent magnetization

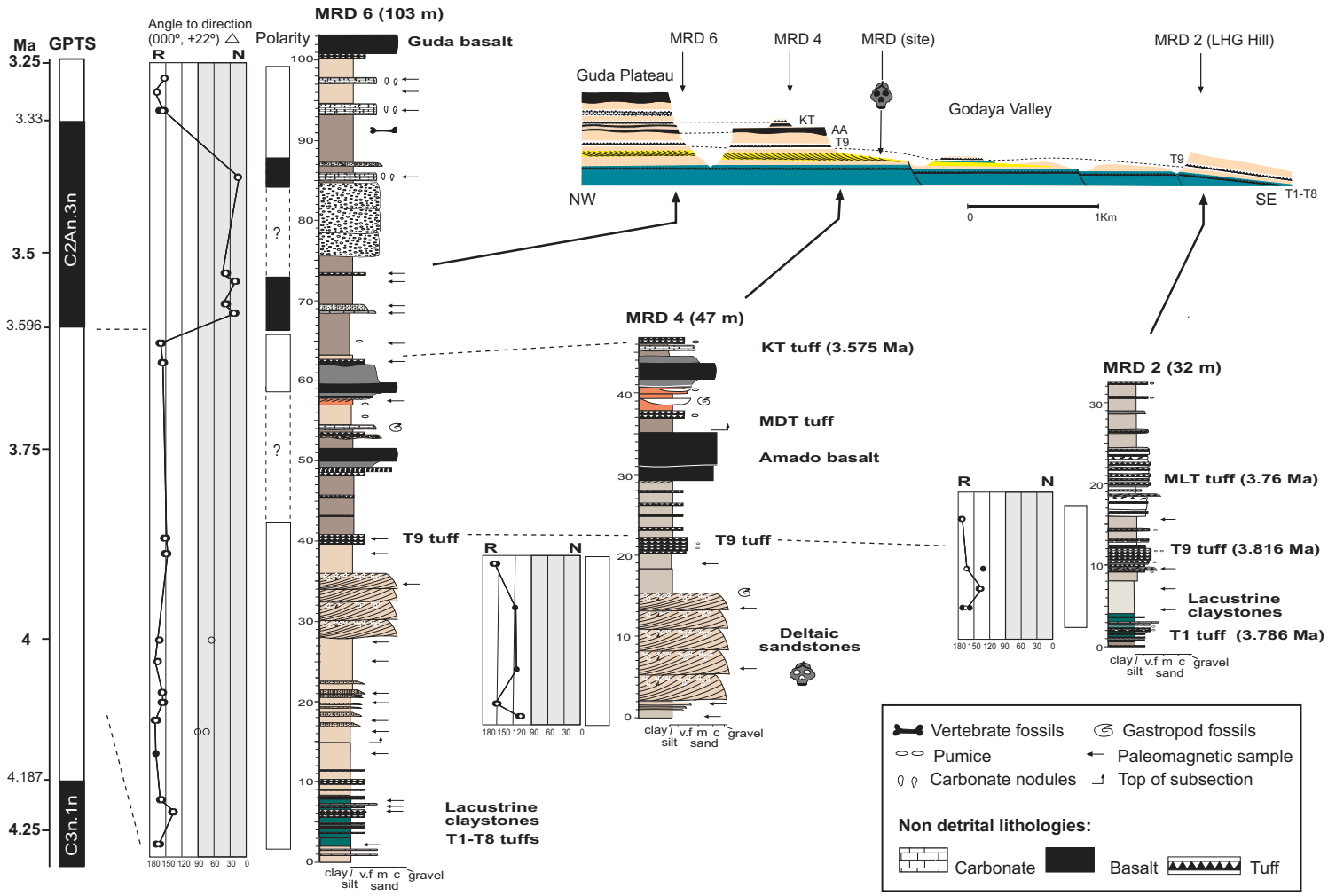

Figure 2 Magnetostratigraphic correlation and geological cross section between the MRD-6 and MRD-2 sections used to constrain the age of the MRD cranium located near the MRD-4 section. Only MRD-6 is long enough to record multiple polarity zones. Key tuff beds, distinguished on the basis of lithology, chemistry, and age, were used to correlate the sections and local polarity with the geomagnetic polarity timescale (Saylor et al. 2019). Remanence directions are displayed as the angle to the expected normal direction (000°, +22°) (After Hoffman (1984)). KT = Kilaytoli Tuff; MDT = Mesgid Dora Tuff; MLT = Mille Tuff; and T1–T9 indicate local informal tuff designations. Modified from Saylor et al. (2019).

histories. However, flat-lying strata are common in some parts of the Rift Valley, where alternative field tests should be performed (see Langereis et al. 2010).

Magnetostratigraphy Example—Dating Australopithecus anamensis *from the Godaya Valley, Afar, Ethiopia*

In 2016, a skull of *Australopithecus anamensis* (MRD-VP-1/1) was discovered in Pliocene sandstones of a deltaic system in the Godaya Valley, Afar region, Ethiopia (Haile-Selassie et al. 2019). A precise age for this significant find (representing the entire craniofacial morphology of the earliest known members of the genus *Australopithecus*) was eventually obtained using a combination of magnetostratigraphy, tephrostratigraphy, and radiometric dating (Saylor et al. 2019).

The first step in this process was to characterize and collect paleomagnetic samples in the relatively short stratigraphic succession in the immediate area of the fossil occurrence (Fig. 3; S4 in Saylor et al. 2019). This information was correlated to a broader stratigraphy, yielding a correlation with tuffs of known age of the Kilaytoli Tuff and the Mille Tuff (Deino et al. 2010), as well as basalt flows that occur farther to the southeast and are geochemically identified as the Am-Ado basalt group (Alene et al. 2017).

With these chronostratigraphic markers, the longest section in the area (S6, ~100 m thick, 1 km from S4) was selected for a more detailed paleomagnetic study (Fig. 3). This section culminated in the widespread, plateau-forming Guda Basalt. Samples were collected from the lowest possible strata to the highest bed. Because S6 occurs in a remote area without roads or water, sampling was done without drilling equipment by collecting oriented blocks. Not all stratigraphic units were useful for sampling, especially in the middle-upper part of the section where sediments were baked by overlying basalt flows, displayed late diagenesis or weathering, or were too coarse-grained.

The volcaniclastic sequence at S6 revealed three polarity zones (R-N-R). Tephrochemical correlations of $^{40}Ar/^{39}Ar$ dated tuffs in S6 from both local and distal exposures within the field area permitted a confident assignment of the polarity sequence to the GPTS; the normal zone was correlated to Chron C2An.3n (3.596–3.33 Ma; Ogg 2020). The MRD skull was found in the reverse polarity region below this normal zone, and thus likely lies within Chron C2Ar (4.187–3.596 Ma). Ultimately, paleomagnetic, radiometric, and tephrochemical data were used in a Bayesian stratigraphic analysis to further constrain the fossil to an age range from 3.804 ± 0.013 Ma to 3.777 ± 0.014 Ma (mean ± 1σ) (Saylor et al. 2019).

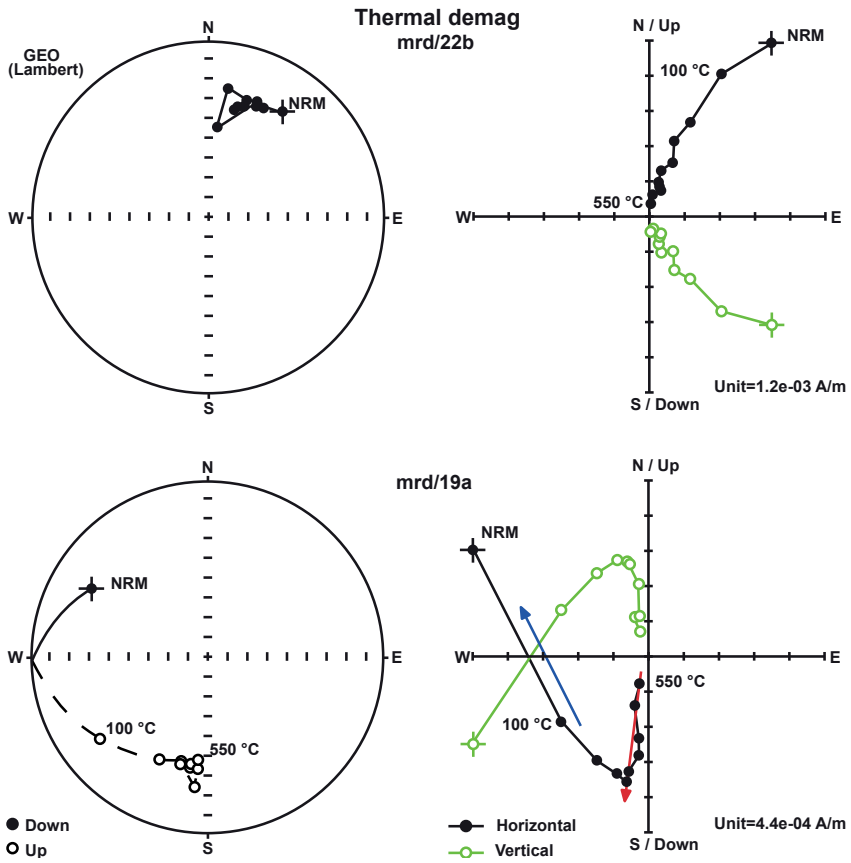

Figure 3 Demagnetization stereoplots (**left**) and Zijderveld diagrams (**right**) for normal (**top**) and reverse (**bottom**) samples from the MRD-6 section. A Zijderveld diagram consists of a projection of the endpoint demagnetization vectors onto orthogonal planes. Here, solid dots represent the projection of the vector onto the horizontal plane (declination values), while open circles (green line) are inclination values projected onto the vertical plane. Notice in the reverse sample a low-temperature component in the magnetization with declination approximately toward the northwest (blue arrow) and the characteristic remanent magnetization (ChRM) with a declination toward the south (190°) expressed at higher temperatures (red arrow). Magnetization is given in A/m (Ampere/meter).

TEPHROSTRATIGRAPHY

Tephrostratigraphy relies on the fingerprinting of volcanic glass in volcanoclastic layers (i.e., tephra horizons or tuffs) to correlate event-stratigraphic horizons across sedimentary archives. The identification and correlation of tephra layers is based on stratigraphic, physical, mineralogical, and geochemical analyses (Lane et al. 2017). In principle, each eruption has a unique chemical signature that is trackable from proximal to distal deposits, but tephra horizons are not always correlated to a known eruption. When correlated regionally, tephra horizons form isochrons that constitute time markers within potentially widely separated stratigraphic sequences. Tephrostratigraphic correlations provide a relative dating approach; when used to extend the applicability of absolute dating techniques, a full chronostratigraphic framework can be developed.

In the East African Rift, tephrostratigraphy has been widely utilized to correlate volcaniclastic strata and has been particularly critical in constraining the ages of hominid fossils and archeological remains (e.g., Clark et al. 2003; WoldeGabriel et al. 2005; Morgan and Renne 2008; Quade and Wynn 2008; Blegen et al. 2016; McHenry et al. 2020; Vidal et al. 2022a). Sedimentary formations in the rift typically contain at least a few intercalated tephra horizons. While radiometric and paleomagnetic dating techniques are often employed where feasible, a regional chronostratigraphic framework cannot rely on these techniques alone; $^{40}Ar/^{39}Ar$ dating, for example, may not be feasible

or sufficiently precise (i.e., fine grain size, young age, or unsuitable mineralogy), or stratigraphic sections may not include a characteristic paleomagnetic reversal pattern. Geochemical tephra correlations can address these issues, but may be impeded by the similarity in major and trace element compositions between eruptive products, from the same volcano or even different volcanoes (e.g., in the Main Ethiopian Rift). This difficulty highlights the importance of (1) combining evidence from the volcanological record and the chronostratigraphy of distal sequences and (2) the analytical methods and array of elements considered when characterizing and correlating samples. Ideally, correlations are based on a detailed suite of major, minor, and trace element single-grain glass shard or pumice glass analyses (Lowe et al. 2017). However, several studies have established tephrostratigraphic correlations based on analyses of purified bulk glass separates (e.g., Clark et al. 2003).

Single-grain Glass Analysis

Single-grain glass analysis should follow the recommendations of the International Focus Group on Tephrochronology (Lane et al. 2017; Lowe et al. 2017) for the geochemical characterization of volcanic glass. Bulk samples of tephra deposits (or tuffs) are sieved under purified water and hydrochloric acid (1%) and then dried. Each grain-size fraction is observed under a microscope to describe its lithology. Altered tuffs with a lower glass fraction may undergo heavy liquid density separation to facilitate the recovery of preserved shards. Samples are either mounted directly into pre-drilled resin mounts, or if sufficiently coarse (>125 µm), glass grains are handpicked under a binocular microscope to select the best grains, which are then mounted in resin stubs. Samples are then polished to electron microprobe analysis (EMPA) standards to expose a flat surface of glass.

Major component abundances of individual glass grains are measured by EMPA. Electron microprobe analysis is an in situ, non-destructive, X-ray spectrometric technique based on the quantitative determination of the elemental composition of solid samples using a microbeam. Where possible, 20 to 30 different glass grains should be analyzed to be representative of the sample's composition and reveal potential compositional heterogeneities. Trace element compositions are measured by laser ablation inductively coupled plasma mass spectrometry (LA-ICP-MS), whereby a laser ablates minute quantities of a sample, which are then ionized into a plasma and transferred to a mass spectrometer detector for elemental analysis. At least approximately 15 of the largest glass shards should be analyzed using LA-ICP-MS, when possible, and more if the sample is heterogeneous. Only shards >10 µm in size can be analyzed, which presents some limitations for cryptotephra (cryptic glass shards invisible to the naked eye) in very distal samples. The analytical accuracy is checked against secondary international standards for both methods.

Purified Bulk Separates Analysis

This method provides the geochemical composition of bulk tuff samples where mineral phases have been removed, such that only the glass fraction is analyzed. Spectroscopic techniques include direct-current plasma atomic absorption, neutron activation, and X-ray fluorescence. Sample purification is achieved through a combination of magnetic and density separations (Katoh et al. 1999). Highly magnetic minerals are first removed from the disaggregated sample with a strong hand magnet. A Frantz isodynamic separator is then used to isolate a relatively non-magnetic glass fraction. Density separations are typically performed using polytungstate solutions to float glass and sink mineral phases. Samples are then examined under a binocular microscope with polarization capability, and remaining mineral grains are removed. Necessary sample sizes for various techniques range from a few hundred milligrams to several grams. The advantage of these bulk techniques is their sensitivity to low-abundance elements and high degree of reproducibility. A serious disadvantage, however, is that tephra deposits may be multimodal in chemical composition, such that this approach is best used following single-shard characterization.

Correlations

Assessment of the geochemical affinity of glass samples can often be confidently achieved based solely on major and trace element bi-plots. A suite of plots allows the internal variability of the datasets to be observed and a visual assessment of the overlap between samples to be made. Additionally, statistical tools such as distance measures, similarity coefficients, hierarchical cluster analysis, and principal component analysis (PCA) on normalized major and trace element datasets can be used to verify bi-plot interpretations and explore the data in multivariate space (Lowe et al. 2017). To avoid miscorrelations resulting from differential alteration and the internal compositional variability of a sample, these tools should be limited to immobile components and those comfortably above the limits of detection of the instrument, e.g., TiO_2, Al_2O_3, FeO, CaO, Y, Zr, Nb, La, Ce, Nd, Hf, Ta, and Th have been used for Main Ethiopian Rift tephra (e.g., Vidal et al. 2022b). Datasets are only comparable if the samples are analyzed using the same analytical procedures and conditions, hence the necessity of standardized practices in a specific geographical region.

Tephrostratigraphy Example—Constraining the Age of the Oldest *Homo sapiens* in Eastern Africa

Tephrostratigraphy was used in combination with $^{40}Ar/^{39}Ar$ dating to constrain the ages of the two oldest *Homo sapiens* fossils in eastern Africa, namely the Omo I and Herto specimens (e.g., Clark et al. 2003; Brown et al. 2012; Vidal et al. 2022a), both found in Ethiopia. The Herto fossils were recovered in the Afar Rift (see Sahle et al. 2019 for a review), preserved in a ~160-ka sandstone within the Upper Herto Member of the Bouri Formation. This sandstone is capped by the Waidedo Vitric Tuff (WAVT), which is widespread across western Afar and identified at Gona, 50 km north of Herto. Direct $^{40}Ar/^{39}Ar$ dating of the WAVT has remained unsuccessful, but the tuff was correlated to tuff TA-55 from the Konso Formation (Fig. 4) in the southern Ethiopian Rift based on major element analyses of individual grains and major and trace element analyses of purified bulk separates (Clark et al. 2003; Hart et al. 2003). In Konso, Unit TA-55 lies below the 155 ± 14 ka (2σ) Silver Tuff (Fig. 4) and its correlation to the Herto WAVT therefore suggests a minimum age of 155 ± 14 ka for the Herto fossils.

The Omo I remains were discovered in the lower Omo Valley of southern Ethiopia (Day et al. 1969), at the surface of a siltstone near the top of Member I of the Kibish Formation. The maximum age of Omo I was initially constrained by the 197 ± 4 ka (2σ) Nakaa'kire Tuff (McDougall et al. 2005). However, the uncertain stratigraphic relationship between this tuff and the fossils permitted ambiguity regarding the age of Omo I (see Vidal et al. 2022a for a review). Much attention was focused on dating the Kamoya Hominin Site (KHS) Tuff that overlies Member I, where Omo I was retrieved (Fig. 4). The fine grain size of the KHS Tuff precluded direct

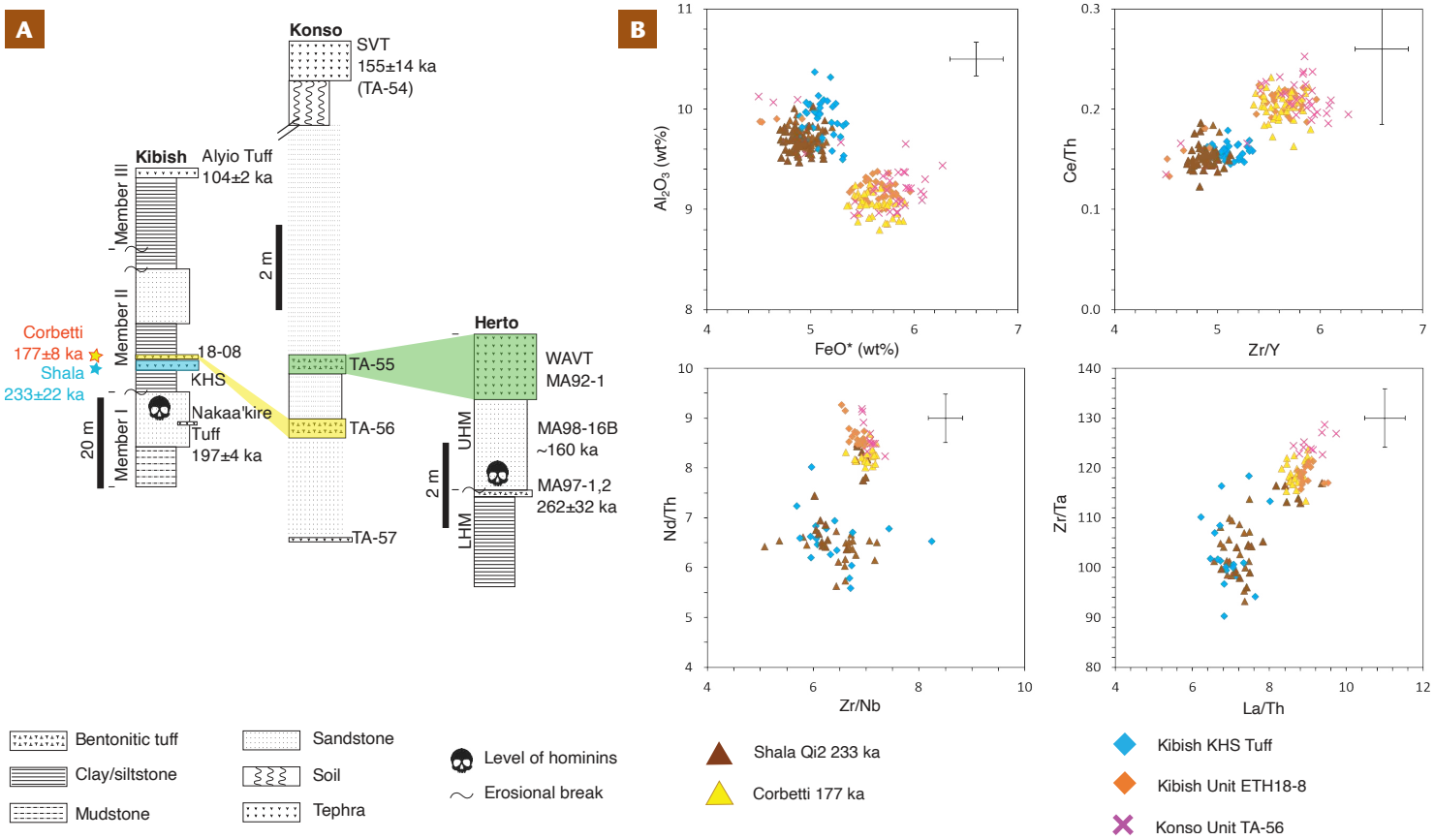

Figure 4 (**A**) Synthetic stratigraphic logs of the Kibish, Konso, and Herto Bouri formations in Ethiopia, showing tephrostratigraphic correlations that provide minimum ages for the *Homo sapiens* fossils Omo I (Vidal et al. 2022a) and Herto (Clark et al. 2003), and source eruptions (stars). SVT = Silver Tuff; KHS = Kamoya's Hominid Site Tuff; LHM = Lower Herto Member; UHM = Upper Herto Member; and WAVT = Waidedo Vitric Tuff. Modified from Vidal et al. (2022a). (**B**) Major element abundances and trace element ratios of glasses from the ca. 233-ka Shala Qi2 eruption, the ca. 177-ka Corbetti eruption, the Kibish KHS and ETH18-8 tuffs, and Konso TA-56 tuffs in (**A**). Major element data are normalized to 100% anhydrous. Error bars shown are relative standard deviations, rescaled to the value of the center point. Published data for the Herto WAVT and Konso TA-55 tuffs are not compared with data plotted here because of the different analytical methods used. Modified from Vidal et al. (2022a).

$^{40}Ar/^{39}Ar$ dating, so tephrostratigraphic correlations with other tephra of the Ethiopian Rift were attempted to provide a minimum age for Omo I (Brown et al. 2012). Comparisons of published major element abundances in glasses from several tuffs of the Main Ethiopian Rift suggested that the KHS Tuff was a correlative of Konso TA-55 and therefore of the Herto WAVT (Brown et al. 2012).

Recently, new analyses of major and trace abundances in the KHS Tuff glasses revealed a convincing correlation with an eruption of the Shala Volcanic Complex in the Main Ethiopian Rift, with an $^{40}Ar/^{39}Ar$ age of 233 ± 22 ka (Vidal et al. 2022a). This tephrostratigraphic correlation provided a revised robust minimum age of ~233 ka for Omo I (Fig. 4). A new tuff found above the KHS Tuff at Kibish was also correlated to Konso unit TA-56, which lies below TA-55, and to a 177 ± 8 ka eruption of the Corbetti Volcano (Fig. 4, Vidal et al. 2022a). This correlation implies that (1) Konso TA-55 is younger than 177 ± 8 ka and therefore cannot be correlated to the KHS Tuff, and that (2) the KHS Tuff and WAVT are from different eruptions. This resolution of tephrostratigraphic questions regarding the age of *Homo sapiens* fossils of the Ethiopian Rift was achieved, despite often subtle geochemical differences among silicic tephra, by the use of large datasets of major and trace elements measured under identical conditions across all samples.

CONCLUSIONS

We illustrated how radiometric dating, magnetostratigraphy, and tephrostratigraphy work together to provide secure age calibrations of hominid fossils and artifacts in the Rift Valley of eastern Africa. $^{40}Ar/^{39}Ar$ dating, while considered a "gold standard" in the absolute dating of Middle–Late Cenozoic rocks where suitable volcanic material can be found, may be hindered by deposits exhibiting too fine a grain size, phenocrysts of low K content, or samples with too young of an age (depending on the K content). Furthermore, the technique is relatively expensive, so it is reasonable to leverage a few high-quality $^{40}Ar/^{39}Ar$ ages by integrating them into a broader chronostratigraphic fabric built via tephro- and magnetostratigraphy. Magnetostratigraphy has the advantage of wide applicability in reasonably fine-grained sedimentary strata but requires absolute age control to anchor short polarity sequences to the GPTS. Finally, tephrostratigraphy may not be universally applicable because of the alteration of glass or grain size constraints and requires absolute age calibration at some point to provide numeric age constraints. However, the three approaches taken together are often successful in facilitating the development of the precise and accurate age control of hominid and artifact-bearing strata in the East African Rift.

REFERENCES

Alene M and 6 coauthors (2017) Geochemistry of Woranso–Mille Pliocene basalts from west-central Afar, Ethiopia: implications for mantle source characteristics and rift evolution. Lithos 282–283: 187-200, doi: 10.1016/j.lithos.2017.03.005

Blegen N and 8 coauthors (2016) The Menengai Tuff: a 36 ka widespread tephra and its chronological relevance to Late Pleistocene human evolution in East Africa. Quaternary Science Reviews 152: 152-168, doi: 10.1016/j.quascirev.2016.09.020

Brown FH, McDougall I, Fleagle JG (2012) Correlation of the KHS Tuff of the Kibish Formation to volcanic ash layers at other sites, and the age of early *Homo sapiens* (Omo I and Omo II). Journal of Human Evolution 63: 577-585, doi: 10.1016/j.jhevol.2012.05.014

Clark JD and 12 coauthors (2003) Stratigraphic, chronological and behavioural contexts of Pleistocene *Homo sapiens* from Middle Awash, Ethiopia. Nature 423: 747-752, doi: 10.1038/nature01670

Day MH (1969) Early *Homo sapiens* remains from the Omo River region of south-west Ethiopia: Omo human skeletal remains. Nature 222: 1135-1138, doi: 10.1038/2221135a0

Deino AL and 5 coauthors (2010) $^{40}Ar/^{39}Ar$ dating, paleomagnetism, and tephrochemistry of Pliocene strata of the hominid-bearing Woranso-Mille area, west-central Afar Rift, Ethiopia. Journal of Human Evolution 58: 111-126, doi: 10.1016/j.jhevol.2009.11.001

Deino AL and 9 coauthors (2021) Chronostratigraphy and age modeling of Pleistocene drill cores from the Olduvai Basin, Tanzania (Olduvai Gorge Coring Project). Palaeogeography, Palaeoclimatology, Palaeoecology 571: 109990, doi: 10.1016/j.palaeo.2020.109990

Evernden JF and 15 coauthors (1965) The potassium-argon dating of Late Cenozoic rocks in East Africa and Italy. Current Anthropology 6: 342-385, doi: 10.1086/200619

Grommé CS, Hay RL (1971) Geomagnetic polarity epochs: age and duration of the Olduvai normal polarity event. Earth and Planetary Science Letters 10: 179-185, doi: 10.1016/0012-821X(71)90004-5

Haile-Selassie Y, Melillo SM, Vazzana A, Benazzi S, Ryan TM (2019) A 3.8-million-year-old hominin cranium from Woranso-Mille, Ethiopia. Nature 573: 214-219, doi: 10.1038/s41586-019-1513-8

Hart WK and 6 coauthors (2003) Dating of the Herto hominin fossils. Nature 426: 622, doi: 10.1038/426622a

Hay RL (1976) Geology of the Olduvai Gorge: A Study of Sedimentation in a Semiarid Basin. University of California Press, 203 pp

Hoffman KA (1984) A method for the display and analysis of transitional paleomagnetic data. Journal of Geophysical Research: Solid Earth 89: 6285-6292, doi: 10.1029/JB089iB07p06285

Katoh S, Danhara T, Hart WK, WoldeGabriel G (1999) Use of sodium polytungstate solution in the purification of volcanic glass shards for bulk chemical analysis. Nature and Human Activities 4: 45-54, doi: 10.24713/nha.4.0_45

Kirschvink JL (1980) The least-squares line and plane and the analysis of palaeomagnetic data. Geophysical Journal International 62: 699-718, doi: 10.1111/j.1365-246X.1980.tb02601.x

Kuiper KF and 5 coauthors (2008) Synchronizing rock clocks of Earth history. Science 320: 500-504, doi: 10.1126/science.1154339

Lane CS, Lowe DJ, Blockley SPE, Suzuki T, Smith VC (2017) Advancing tephrochronology as a global dating tool: applications in volcanology, archaeology, and palaeoclimatic research. Quaternary Geochronology 40: 1-7, doi: 10.1016/j.quageo.2017.04.003

Langereis CG, Krijgsman W, Muttoni G, Menning M (2010) Magnetostratigraphy concepts, definitions, and applications. Newsletters on Stratigraphy 43: 207-233, doi: 10.1127/0078-0421/2010/0043-0207

Leakey LSB, Evernden JF, Curtis GH (1961) Age of Bed I, Olduvai Gorge, Tanganyika. Nature 191: 478-479, doi: 10.1038/191478a0

Lowe DJ and 5 coauthors (2017) Correlating tephras and cryptotephras using glass compositional analyses and numerical and statistical methods: review and evaluation. Quaternary Science Reviews 175: 1-44, doi: 10.1016/j.quascirev.2017.08.003

Lowrie W (1990) Identification of ferromagnetic minerals in a rock by coercivity and unblocking temperature properties. Geophysical Research Letters 17: 159-162, doi: 10.1029/GL017i002p00159

McDougall I, Brown FH, Fleagle JG (2005) Stratigraphic placement and age of modern humans from Kibish, Ethiopia. Nature 433: 733-736, doi: 10.1038/nature03258

McDougall I, Harrison TM (1999) Geochronology and Thermochronology by the $^{40}Ar/^{39}Ar$ Method (Second Edition). Oxford University Press, 269 pp, doi: 10.1093/petrology/41.12.1823

McHenry LJ and 5 coauthors (2020) Tuff fingerprinting and correlations between OGCP cores and outcrops for Pre-Bed I and Beds I/II at Olduvai Gorge, Tanzania. Palaeogeography, Palaeoclimatology, Palaeoecology 548: 109630, doi: 10.1016/j.palaeo.2020.109630

Morgan LE, Renne PR (2008) Diachronous dawn of Africa's Middle Stone Age: new $^{40}Ar/^{39}Ar$ ages from the Ethiopian Rift. Geology 36: 967-970, doi: 10.1130/G25213A.1

Niespolo EM, Rutte D, Deino AL, Renne PR (2017) Intercalibration and age of the Alder Creek sanidine $^{40}Ar/^{39}Ar$ standard. Quaternary Geochronology 39: 205-213, doi: 10.1016/j.quageo.2016.09.004

Ogg JG (2020) Geomagnetic polarity time scale. In: Gradstein FM, Ogg JG, Schmitz MD, Ogg GM (eds) Geologic Time Scale 2020. Elsevier, Amsterdam, pp 159-192, doi: 10.1016/B978-0-12-824360-2.00005-X

Quade J, Wynn JG (2008) The geology of early humans in the Horn of Africa. Geological Society of America Special Paper 446, 234 pp, doi: 10.1130/SPE446

Sahle Y and 9 coauthors (2019) Revisiting Herto: new evidence of *Homo sapiens* from Ethiopia. In: Sahle Y, Reyes-Centeno H, Bentz (eds) Modern Human Origins and Dispersal. Kerns Verlag, Tübingen, pp 73-104

Saylor BZ and 13 coauthors (2019) Age and context of mid-Pliocene hominin cranium from Woranso-Mille, Ethiopia. Nature 573: 220-224, doi: 10.1038/s41586-019-1514-7

Stanistreet IG and 6 coauthors (2020) New Olduvai Basin stratigraphy and stratigraphic concepts revealed by OGCP cores into the Palaeolake Olduvai depocentre, Tanzania. Palaeogeography, Palaeoclimatology, Palaeoecology 554: 109751, doi: 10.1016/j.palaeo.2020.109751

Vidal CM and 11 coauthors (2022a) Age of the oldest known *Homo sapiens* from eastern Africa. Nature 601: 579-583, doi: 10.1038/s41586-021-04275-8

Vidal CM and 16 coauthors (2022b) Geochronology and glass geochemistry of major Pleistocene eruptions in the Main Ethiopian Rift: towards a regional tephrostratigraphy. Quaternary Science Reviews 290: 107601, doi: 10.1016/j.quascirev.2022.107601

WoldeGabriel G, Hart WK, Katoh S, Beyene Y, Suwa G (2005) Correlation of Plio–Pleistocene tephra in Ethiopian and Kenyan rift basins: temporal calibration of geological features and hominid fossil records. Journal of Volcanology and Geothermal Research 147: 81-108, doi: 10.1016/j.jvolgeores.2005.03.008

Zijderveld JDA (1967) A. C. demagnetization of rocks: analysis of results. In: Collinson DW, Creer KM, Runcorn SK (eds) Methods in Palaeomagnetism. Elsevier, Amsterdam, pp 254-286 ■